

# An Overview of Rheology in the Computer Industry

T. E. KARIS

IBM Research Division, Almaden Research Center, 650 Harry Road, San Jose, California 95120-6099

## SYNOPSIS

The rheological characterization of a wide variety of materials used in computer hardware is described. The materials and applications presented include liquid crystal polymers for components, solder paste for surface mounting of integrated circuits, screen printable polyimide for dielectric patterns, new photosensitive polyimide to reduce processing steps, hot-melt adhesive for temporary bonding, pressure-sensitive adhesive for permanent bonding of optical recording disks, bearing grease for magnetic recording disk drive spindles, fluoropolymer lubricants for magnetic recording disks, magnetic particle suspensions for magnetic tape and disks, toner for laser printing, thermoplastic polymer for rapid prototyping, and cathode paste for rechargeable lithium batteries. Rheological tests appropriate for each of the materials were designed to provide key information about its performance in the intended application. This overview provides insight into the relation between interpretation of rheological test data and materials performance in engineering applications as well as for process control. Rheology is essential to the development of computer hardware and peripheral devices. © 1996 John Wiley & Sons, Inc.

## INTRODUCTION

Modern computer systems include a system unit, data storage retrieval, and input/output devices. The system unit incorporates circuit cards and integrated circuit chips. Advanced liquid crystal polymers are being explored for use as circuit cards and other components. Integrated circuit chips (ICs) cards are electrically connected by solder paste screened through a pattern onto the circuit cards in surface mount technology. Insulating layers with micron and submicron scale features are formed on boards and wafers using an advanced photosensitive polymer. During micromachining, small parts are held in place by a soluble hot-melt adhesive. Magneto-optical recording disks are held together by a pressure-sensitive adhesive that must maintain dimensional stability over the projected disk lifetime. Grease is employed to lubricate the bearings on the shaft of magnetic recording disk drives. Fluoropolymer lubricants protect magnetic recording disks during start and stopping. Magnetic recording tape and

floppy disks are made by coating with a suspension of magnetic particles. In laser printing, toner is melted and fused into the paper to form the printed images. In a new type of printing, called rapid prototyping, a thermoplastic polymer melt is extruded to form a printout of three-dimensional images. Fabrication of high-energy density rechargeable batteries for portable computers requires a precision coating application of microns-thick electrode and electrolyte layers. Each of these materials must have certain rheological properties for processing and to meet their field performance requirements. Their rheology must be well understood to ensure product reliability and to advance new and improved materials for future products. This article describes rheological studies on these materials.

The first step in the rheological characterization of a material is to determine the appropriate rheological test apparatus. In these studies, applied stress or applied strain measurements with 25.4 or 50 mm-diameter cone-on-plate (1–3° cone angle), or parallel-plate, fixtures were employed. The rheometers used were (1) a Rheometrics RMS705 mechanical spectrometer with 2000 g-cm transducer and melt oven, (2) a Rheometrics fluids rheometer with 100

g-cm transducer, and (3) a Carrimed (now TA Instruments) CSL500 stress rheometer. An environmental chamber is necessary to achieve a temperature range from  $-100$  to  $400^{\circ}\text{C}$  for temperature-frequency sweeps and time-temperature superposition. The second step in characterizing a new material is to determine the appropriate test for measuring rheological properties relevant to the materials' intended application. The tests presented here include temperature sweep, oscillation frequency sweep, steady shear, thixotropic loop, and creep. Unless otherwise specified, the strain amplitude was 1% and temperature sweeps were done at an oscillation frequency of 10 rad/s.

## CASE STUDIES

### Liquid Crystal Polymer Components

Recently, much interest has focused on liquid crystal polymers (LCPs) for interconnects, circuit cards, and slider load/unload ramps in disk drives. LCPs useful for these applications are processable as thermoplastics, display low creep at elevated use temperatures, and have a low dielectric constant. One LCP candidate that we examined was a copolymer of *p*-hydroxybenzoic acid/poly(ethylene terephthalate), referred to as LCPTE. Extensive melt rheological studies on this copolymer were done in our laboratory and elsewhere.<sup>1</sup> The key finding was that of a reversible increase in the storage modulus during annealing of the melt. The LCPTE was inappropriate for this application because of outgassing, dimensional instabilities due to residual stress relaxation, and polymer flow orientation.

New LCP molecular structures were developed with improved LCP performance. One of the new LCPs was tested in our laboratory.<sup>2</sup> This LCP was a copolymer of 6-hydroxy-2-naphthoic acid/*p*-hydroxybenzoic acid/terephthalic acid/4-4'-biphenol, referred to here as LCPVE. The key rheological features of this copolymer at  $380^{\circ}\text{C}$  are illustrated by the storage modulus as a function of oscillation frequency in Figure 1. The filled circles show the somewhat fluidlike melt properties of the unannealed material. In the unannealed state, the LCPVE can be injection- or compression-molded and exhibits dramatic shear thinning. After annealing at  $300^{\circ}\text{C}$  for 8 h (filled squares) or 43 h (filled triangles), the LCPVE is much more solidlike. In this state, the LCPVE cannot be made to flow at any temperature, and nematic properties have disappeared. The test

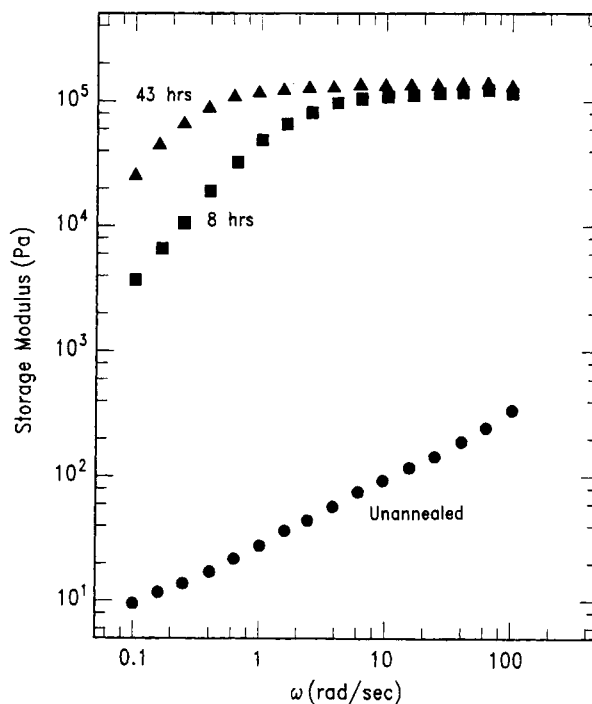


**Figure 1** The storage shear modulus at  $380^{\circ}\text{C}$  as a function of oscillation frequency for LCPVE unannealed and annealed for 8 h or 43 h at  $300^{\circ}\text{C}$ .

temperature was above the annealing temperature, which shows that the annealing is irreversible, in contrast to reversible annealing observed with the LCPTE. Using X-ray diffraction, dielectric measurements, solubility, differential scanning calorimetry, and hot-stage microscopy, the irreversible annealing of LCPVE was determined to result from an increase in the molecular weight of the copolymer.<sup>2</sup> There is the opportunity to form the unannealed LCPVE into parts by injection molding. The parts can subsequently be annealed into nonmelting parts which are dimensionally stable up to nearly  $400^{\circ}\text{C}$ .

### Solder Paste

Surface-mounted ICs are bonded and electrically connected to their pads by solder. Small islands of solder paste are deposited on the circuit card, and the weld to the IC pads is formed by vapor phase heating above the melting point of the lead/tin alloy. Solder paste is a concentrated particle suspension consisting of 90 wt % lead/tin alloy particles 25–45  $\mu\text{m}$  in diameter in a flux consisting of polymers, solvents, surfactants, flow-control agents, and other additives. The pattern of solder paste is deposited

on the circuit card by a process similar to silk screening. Flow and recovery properties of the solder paste determine its ability to precisely form the pattern with edge definition on the order of microns. Solder paste rheology is typically characterized by a single-point viscosity measurement, which is inadequate for predicting higher-performance requirements. We carried out a study aimed at relating the screening performance with the rheological properties using a variety of commercial solder pastes.<sup>3</sup> The rheological tests used were the (1) oscillation frequency sweep, (2) strain amplitude sweep, (3) oscillatory shear as a function of time following cessation of steady shear, and (4) thixotropic loop. The solder pastes were deposited on a test pattern to evaluate their screening performance. The rheological test results were compared with the performance of each paste. The performance was qualitatively predicted by the modulus corresponding to the longest relaxation time  $G_1$  determined from an oscillation frequency sweep. The range of screening speeds increased with decreasing  $G_1$ . The printability was better for pastes which showed less recovery of the dynamic storage modulus following shear. Another indicator of the solder paste performance was the minimum viscosity obtained in the thixotropic loop test as the shear rate was linearly increased to 30 1/s over 60 s time. An example of the thixotropic loop test results on two solder pastes is shown in Figure 2. The data from a paste with poor screening performance are shown by the squares, and the data from a paste with acceptable screening performance are shown by the circles. Further work is required to establish the relation between the rheological properties and the microstructure of the solder paste.

### Screen Printable Polyimide

Polyimide is widely employed as an insulating layer in electronic circuit fabrication.<sup>4</sup> In the conventional process described below, a solution of the polyimide in a volatile solvent is spin-coated onto a substrate such as silicon. The film is dried, overcoated with a thin film of photoresist, and dried again. The photoresist is exposed to irradiation through a mask containing a pattern. Where the photoresist has been exposed, it is soluble and is washed away. The polyimide is thus removed from the regions where the photoresist was exposed. The remaining photoresist is stripped from the polyimide, and the polyimide is cured. As a result, the substrate is coated with polyimide in an insulating pattern containing

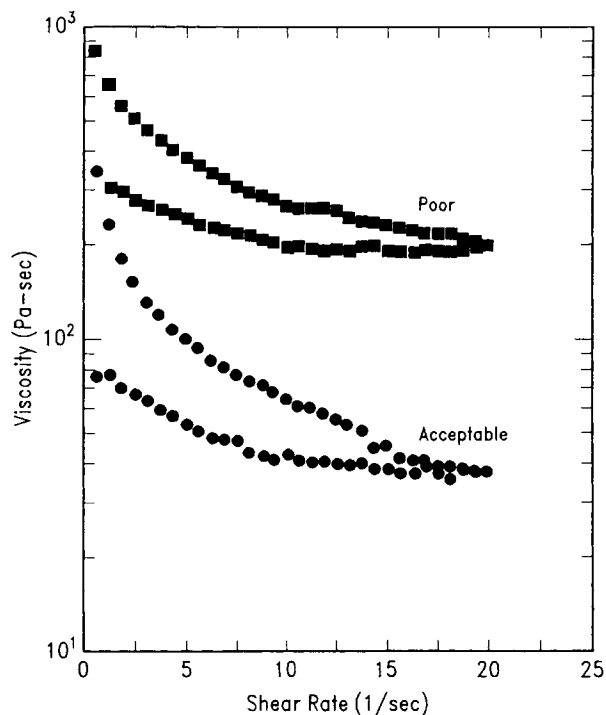


**Figure 2** The viscosity as a function of shear rate in the thixotropic loop test on solder paste: poor screening performance (filled squares); acceptable screening performance (filled circles).

channels for metal deposition on the substrate. The conventional process requires at least six separate steps. A screen printable polyimide is being developed to reduce the number of process steps needed to form the patterns. Screen printing deposits the polyimide directly as lines or patterns which are then cured. A thixotropic polyimide paste is achieved by incorporating polyimide particles in a solvent and binder system.<sup>4</sup> This provides a polyimide film that is relatively free of pinholes.

A filled polyimide composite is used for protection of memory chips from alpha particles.<sup>5</sup> In the application of screen printable polyimide for alpha-particle protection, the polyimide particle suspension is screen printed over the chip surface to form a protective coating. The protective coating should be free of pinholes, and the particle suspension must be sufficiently thixotropic in order to have acceptable screening performance. The pinhole density and the thixotropic index are a function of the filler particle size, as shown in Figure 3 (from Ref. 5). The thixotropic index is the ratio of the viscosity at low shear rate to the viscosity at 10 $\times$  higher shear rate. Decreasing the particle size below 10 microns minimizes the number of pinhole defects and improves

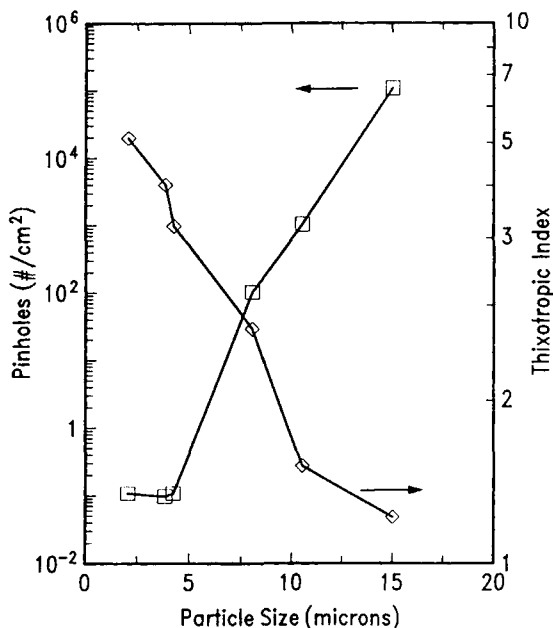


**Figure 3** Screen printable polyimide showing the effect of particle size on pinhole defects and thixotropic index (ratio of low shear viscosity at  $10\times$  higher shear rate) data from Ref. 5.

the screening performance, with the best formulation containing particles smaller than 5 microns.

### Photosensitive Polyimide

A photosensitive polyimide formulation was developed as another way of reducing the number of process steps needed to form the insulating pattern. The photosensitive polyimide incorporates unsaturated bonds in a side chain. The new formulation includes a trifunctional crosslinker, free-radical initiator, and sensitizer. Exposure of the formulation to light initiates a localized free-radical reaction, crosslinking the polyimide, and rendering it insoluble where exposed. The shortened process consists of spin coating the polyimide on a substrate, exposing the pattern, and washing away the unexposed material. Since the new formulation contained unsaturated bonds, rheological tests were done to evaluate the shelf-life stability in case there was any crosslinking during storage. An oscillation frequency sweep test was employed. Figure 4 shows the oscillatory shear moduli of a freshly prepared formulation (circles), after 30 days storage (squares), and after 60 days storage (triangles). The storage modulus is indicated by open symbols, and the loss modulus, by filled symbols. There was no detectable change

in the rheology of the formulation during storage. These results demonstrated that the new photosensitive polyimide formulation could be stored for long enough periods of time during use in a manufacturing environment.

### Temporary Bonding

To perform a precision machining operation on certain small parts such as ceramic magnetic recording head slider rows, they are temporarily bonded onto a metal alignment block. A polyamide melt adhesive is extruded in thin lines through nozzles onto the ceramic wafers. The wafers are bonded onto the metal alignment block by heating above the melting temperature of the adhesive. After machining, the adhesive is removed in a solvent bath. A study was done to optimize the melting temperature, melt viscosity, and dissolution rate by blending two grades of the adhesive. Grade A had a low melting temperature, high melt viscosity, and low dissolution rate, while grade B had a high melting temperature, low viscosity, and high dissolution rate. Figure 5(a) shows the loss modulus as a function of temperature measured on a series of blends, illustrating that the melting temperature and melt viscosity can be controlled by blending. The dissolution rate also changes by an order of magnitude over the range of blend composition. The dissolution rate was compared with the melt viscosity  $\eta$  because both of these properties are related to the long-range motion of polymer chains through the diffusion coefficient  $D \propto 1/\eta$ . Figure 5(b) shows the dissolution rate of the blends as a function of  $1/\eta$  at  $150^\circ\text{C}$ . The dissolution tests were done on powder without stirring. The filled circles in Figure 5(b) show the average dissolution rate after a 36 min heat/cool cycle. The filled squares in Figure 5(b) show the initial dissolution rate measured at room temperature. At the lower melt viscosities (higher  $1/\eta$ ), both the average and initial dissolution rates reached a maximum value. The maximum in the dissolution rate vs.  $1/\eta$  in the limit of low  $\eta$  is consistent with the dissolution rate becoming limited by diffusion through a concentration boundary layer at the interface between the solid polymer particles and the solvent. At the higher melt viscosities (lower  $1/\eta$ ), the initial dissolution rate is nearly proportional to  $1/\eta$ , consistent with the dissolution rate becoming limited by diffusion through the bulk of the solid polymer particles. These studies assisted in specifying a blend with the right combination of melting temperature, melt vis-

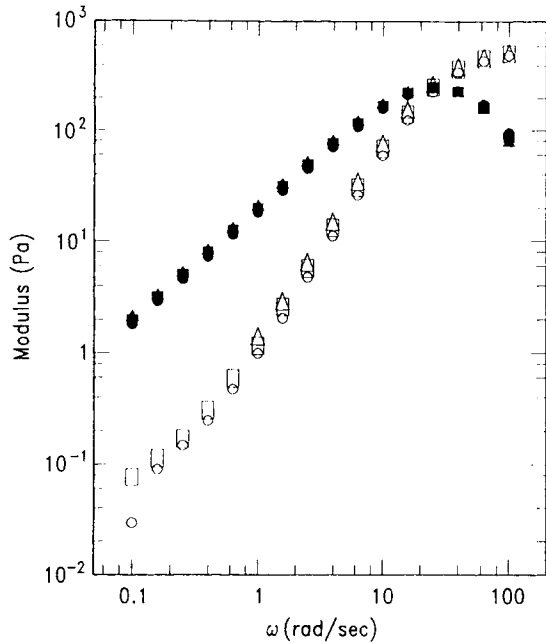


**Figure 4** The shear moduli as a function of oscillation frequency for photosensitive polyimide formulation: storage modulus (open symbols); loss modulus (filled symbols). Initial test (circles); after 30 days (squares); after 60 days (triangles).

cosity, and dissolution rate for use in the manufacturing process.

### Permanent Bonding

Magneto-optical recording disk substrates are made by injection molding polycarbonate. A magneto-optic (MO) layer is deposited on one side of the substrate to record the data. The read/write laser is incident on the MO layer from the uncoated side of the substrate. In the manufacturing of double-sided MO recording disks, two substrates are bonded together with the uncoated sides facing out, hubbed, and placed in a cartridge. The adhesive used for bonding is a thermoplastic blend of polystyrene and ethylene/propylene copolymer. The adhesive melt is deposited in a thin film on the substrates. The substrates are allowed to cool, and then they are pressed together to form double-sided disks. During process development, some of the double-sided disks were found to creep unacceptably (warp) after accelerated life testing at 80°C for 500 h. Oscillatory shear modulus measurements were done on the adhesive used for bonding to determine the time-temperature shift factor. The master curve is shown in Figure 6(a). The adhesive was thermorheologically simple, so

time-temperature superposition could be applied. The time-temperature shift factor relative to 70°C is shown in Figure 6(b), and the smooth curve is a least-squares fit to the WLF equation. Creep tests were also done using a stress rheometer. These indicated that the creep compliance was linear for a reduced time longer than  $10^4$  s. The disk life before the appearance of unacceptable creep was calculated from these rheological test data. The predicted lifetime before failure due to creep of the adhesive was 5000 h at 70°C and 162 years at 50°C.

### Bearing Grease

Rheological measurements were done on the grease used for the ball bearings in disk drive spindles to determine if there was any effect of exposure to high humidity during ship/store conditions on the grease mechanical properties. Numerous studies on grease rheology have been published, e.g., Ref. 6. Grease has complicated rheological properties that depend on shear history, strain amplitude, and rate of strain. Grease comprises a thickener and light lubricating oil. In the grease that we tested, the thickener consisted of rape seed oil saponified with NaOH. The thickener and light oil form concentrated micellar structures which are deformable and often rodlike, providing the grease with a yield stress. At high strain amplitude in oscillatory shear, the light oil forms a surface layer on the grease, so that beyond the yield strain, shear occurs in a thin layer near the surface of the test fixtures. A 1% strain was sufficiently small to propagate the strain through the bulk of the grease sample without exceeding the yield strain. Figure 7 shows the shear moduli of the untreated grease at 23°C (circles), untreated grease at 80°C (squares), and grease equilibrated at 97% relative humidity, dried at 11% relative humidity, and tested at 23°C (triangles). The storage modulus measured at 23°C following the wet/dry cycle approaches the curve measured at 80°C, and the loss modulus measured at 23°C following the wet/dry cycle is nearly the same as that measured at 80°C. The effect of exposure to high humidity on the moduli of the grease that we tested was comparable to that of increasing the temperature. Synthetic grease, which is hydrophobic, is now used in all disk drive spindle ball bearings.

### Magnetic Recording Disk Lubricants

In magnetic recording disk drives, data are stored and retrieved by a ceramic read/write slider. The

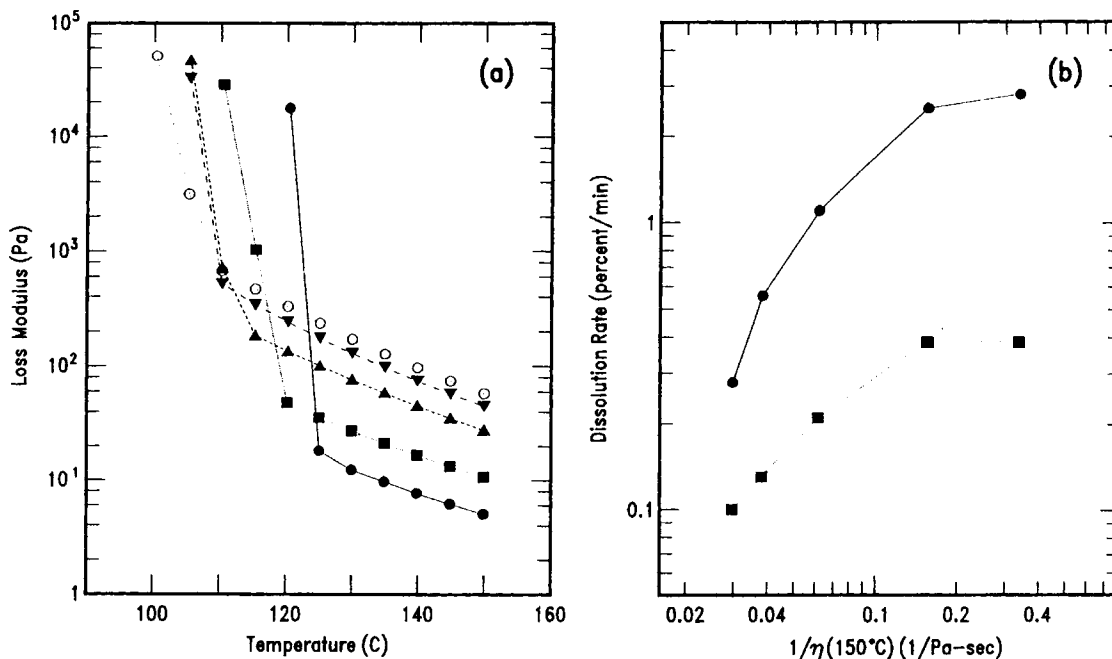


**Figure 5** (a) The loss modulus as a function of temperature for the polyamide blends, grade B/grade A: pure grade B (open circles); 90% grade B (upside down triangles); 70% (right side up triangles); 50% (squares); pure grade A (filled circles). (b) The dissolution rate vs. inverse viscosity for the polyamide blends. Initial dissolution rate at room temperature (squares); average dissolution rate after 36 min heat/cool cycle (circles).

slider is maintained approximately 100 nm above the surface of the spinning disk on a film of air (air bearing). When the disk drive is turned on or off, the slider comes into sliding contact with the disk surface. A molecularly thin (1–2 nm) layer of fluoropolymer lubricant on the disk surface prevents wear during the start/stop cycle. Since the contacts between the slider and the disk occur when the relative velocity between the read/write slider and the disk surface is on the order of 1 m/s, the shear rates on the lubricant film are expected to be on the order of  $10^{10}$  1/s during start/stop. Rheological tests were done on two of the most widely used magnetic recording disk lubricants to obtain the shear moduli at high frequency from the master curve. The two fluoropolymer magnetic recording disk lubricants examined were a Y and a Z structure.<sup>7</sup> Oscillation frequency sweep measurements were done from room temperature down to nearly the glass transition temperature and the data were shifted to obtain the master curves shown in Figure 8. From these data, both of the lubricants are “solidlike” or “glassy” at shear rates above  $10^5$  1/s. The master curve was used to calculate the characteristic time  $\tau_c$ . The  $\tau_c$  for the Y was 30 times longer than that

for the Z lubricant. It is also reported that the Y undergoes more rapid decomposition than does the Z lubricant during steady sliding of the slider on the disk.<sup>7</sup> It may be that the Z molecular structure with the shorter  $\tau_c$  can more easily deform in response to slider disk contacts than can the Y lubricant. Thus, the Z is less susceptible to mechanochemical scission than is the Y lubricant. These rheological test results provided insight into the performance of magnetic recording disk lubricants.

### Magnetic Particle Suspensions

Modern thin-film magnetic recording disks store information as magnetized domains in a sputtered metallic film. Prior to the genesis of the thin-film magnetic recording disk, the magnetized domains on magnetic recording disks were formed in films containing rodlike single-domain magnetic particles in a crosslinked polymer matrix, referred to as particulate media. Floppy disks, tapes, and magnetic stripes still employ the particulate media. The particulate magnetic film is prepared by dispersing iron oxide or chromium oxide or barium ferrite particles in a solution of epoxy-phenolic or polyurethane

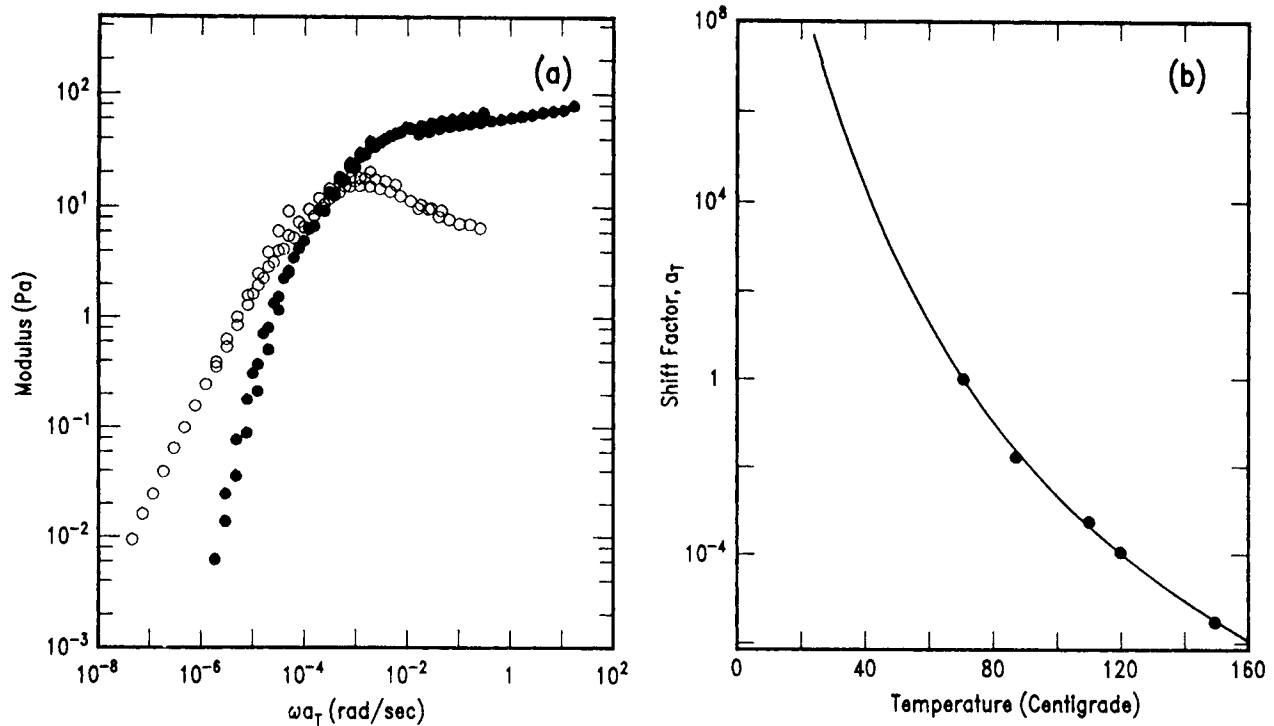


**Figure 6** (a) The master curve for the pressure-sensitive adhesive relative to 70°C: storage modulus (filled symbols); loss modulus (open symbols). (b) The shift factor for the pressure-sensitive adhesive relative to 70°C. The smooth curve is from a regression fit to the WLF equation.

binder resins, solvents, surfactants, and other additives. The magnetic particles are dispersed in a media mill. This magnetic particle suspension is then held in stirred vats for extended periods of time while it is being coated onto the substrates. In the case of rigid disks, the suspension is spin-coated. In the case of floppy disks and tape, the suspension is roll coated onto a web. Following the coating process, the media is heated to drive off volatile solvents and to crosslink the polymer binder. The media is then smoothed by calendaring (for tapes and floppy disks) or by abrasive polishing (for rigid disks), and lubricant is applied. One of the prerequisites for magnetic recording films with high signal-to-noise ratio and squareness of the magnetic hysteresis loop is good magnetic particle dispersion quality (absence of flocculation). Since the suspended particles are magnetic, there are strong attractive forces which tend to flocculate the suspension. The suspension must be well dispersed during the milling process, so that the milling conditions and time are experimentally determined to provide adequate dispersion quality. Excessive milling can break the single-domain magnetic particles into useless subdomain

fragments. After milling and during storage while coating media, adequate dispersion quality must be maintained by stirring and recirculation. For many years, the only way to determine whether or not the dispersion quality was adequate was to evaluate the performance of the final product. This was only possible after significant value had been added to finish the film. Shear viscosity can, in principle, provide a relative measure for the degree of suspension flocculation. Flow alignment of suspended magnetic particles shows up as a decrease in viscosity with increasing shear rate. Figure 9(a) shows the shear viscosity  $\eta$  of a rodlike magnetic particle suspension as a function of step changes in shear rate between 400 and 100 1/s. In Figure 9(a), the sequence of shear rates is high, low, high, low.  $\eta_s$  is the viscosity of the suspending fluid and  $\phi$  is the volume fraction of magnetic particles, usually 1–5%. The rheological measurement of viscosity was inadequate for single-domain magnetic particle dispersion quality measurement because of their rapid flocculation. Dispersion quality off a sample taken off-line for measurement was significantly different from the dispersion quality on the production line.

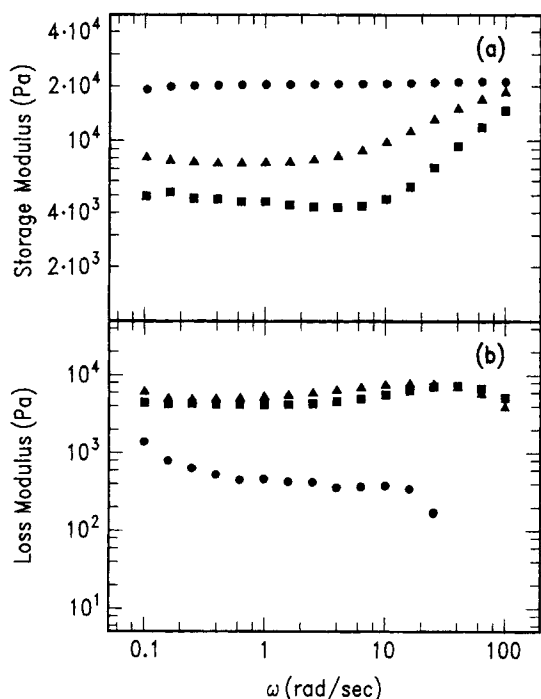


**Figure 7** The shear moduli of a sodium soap thickener/mineral oil grease: (a) storage modulus; (b) loss modulus. Untreated grease at 23°C (circles); untreated grease at 80°C (squares); wet/dry cycled grease at 23°C (triangles).

Much research was focused on developing measurement techniques to characterize the dispersion quality on-line in real-time before further value was added to finish magnetic films made with flocculated magnetic particle suspension. The culmination of this research was an electromagnetic (rheomagnetic) apparatus for measuring the flow alignment of the rod- or platelike magnetic particles. The essence of the rheomagnetic apparatus is a converging flow cell containing a solenoid-shaped measurement coil wound on a glass tube just downstream from the convergence. The weak magnetic sensing field of the coil is mostly parallel to the flow direction. For rod-like single-domain particles, the principle of operation is as follows: When the particle's major axis aligns parallel to the extensional flow field, the coil inductance decreases due to the dependence of a particle's magnetic susceptibility on the orientation angle with respect to the external magnetic field. With decreasing flow rate, the particle alignment becomes more nearly random and the coil inductance increases. The coil inductance is calculated from the frequency of a 1–10 MHz oscillator with the coil as its inductor. Figure 9(b) shows the coil inductance  $L$  during step changes in the flow rate

between 2 and 12 mL/s using the same suspension. In Figure 9(b), the sequence of flow rates is high, low, high, low, high.  $L_s$  is the coil inductance in the absence of magnetic particles. The degree of alignment provides a measure of the flocculation state, or dispersion quality, of the suspended particles. The coil inductance as a function of flow rate is determined by the effective particle shape through the rotary Peclet number  $Pe$ .<sup>8</sup> The  $Pe$  is the ratio of the convective to the diffusive contributions to the rotation of particles (or flocculates) in the flow field. Since flocculates are more nearly spherical than are the rodlike primary particles, the orientation of flocculated primary particles is randomized because they are tumbling rather than aligned in the magnetic field of the coil. Consequently, the measurement of the flow-orientation curve provides an on-line dispersion quality measurement. The rheomagnetic apparatus was successfully used in production of high-quality particulate magnetic recording media.<sup>9</sup>

### Toner for Laser Printing

Laser printing is completed by calendaring toner particles with a heated fuser roll after the toner is

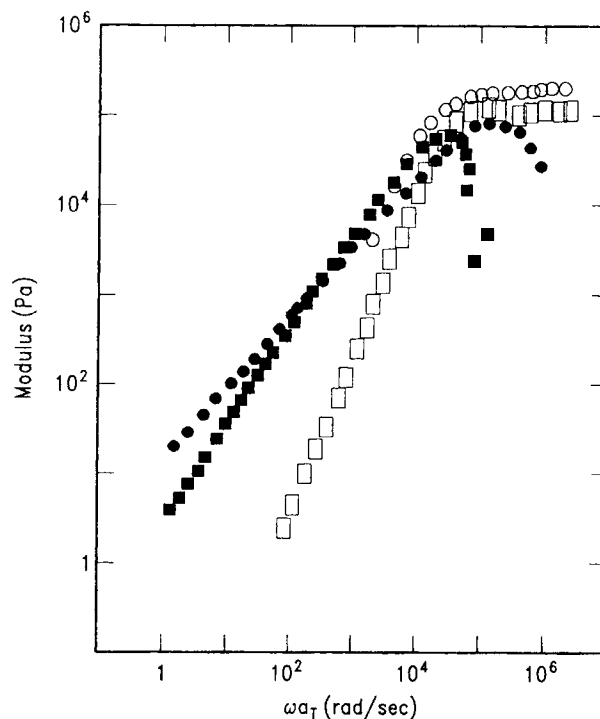


**Figure 8** The master curves of two fluoropolymer lubricants for magnetic recording disks: storage modulus (open symbols); loss modulus (filled symbols); Y lubricant, (squares); Z lubricant (circles).



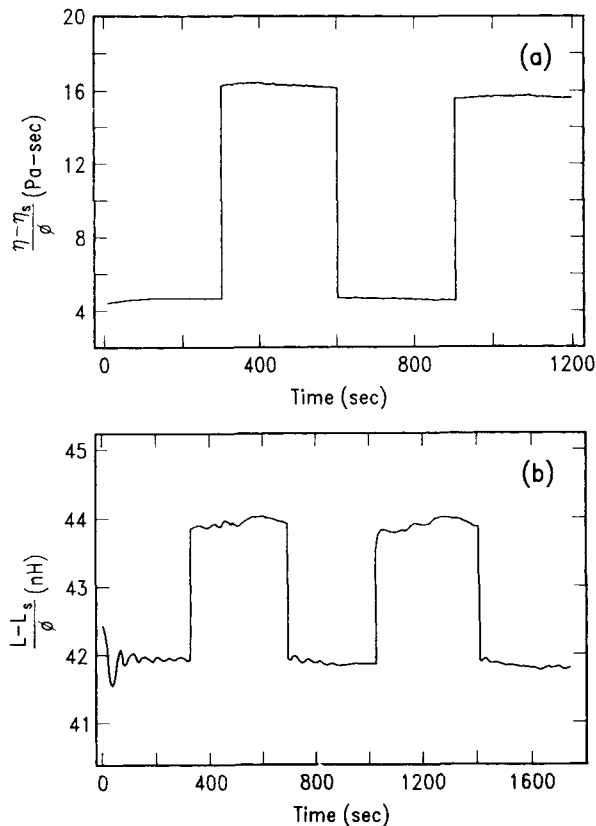


**Figure 9** (a) The viscosity response to step changes in the shear rate; (b) the coil inductance response to step changes in the flow rate for a rodlike single-domain magnetic particle suspension.

deposited on the paper in the pattern of the printed image. Toner is a carbon black-filled thermoplastic polymer resin. A typical toner resin is styrene/butylacrylate/divinylbenzene (68/30/2) copolymer, with the initial degree of crosslinking determined by the amount of divinylbenzene. The amount of divinylbenzene in the copolymer is small, and crosslinking is maintained below the gel point. During preparation, toner is compounded in melt-mixing extruders in which the high shear rate degrades some of the gel, thus determining the viscoelastic properties of the toner. The viscoelastic properties of the toner melt must be appropriate for the speed at which the paper goes through the roller, or the pages per minute. The time in the roller nip  $t_0$  and the characteristic time of the melt  $\tau_c$  combine to form a Deborah number  $De = \tau_c/t_0$ . At low  $De$ , the melt flows, while at high  $De$ , the melt behaves as a solid. The  $De$  for adequate fusing is approximately 9. The recoverable compliance  $J_e^0$  also influences the per-

manent deformation of the toner particles. Both  $\tau_c$  and  $J_e^0$  are controlled by the amount of gel in the toner resin.<sup>10</sup> We studied the effect of processing time on the toner melt rheological properties using an internal mixing rheometer with 50 g capacity. Toner was processed for various amounts of time at 180°C and 80 rpm, and the melt rheological properties were measured 160°C [Fig. 10(a) and (b)]. Both  $\tau_c$  and  $J_e^0$  decreased with increased processing time.

Proper adhesion of the toner also plays an essential role in laser printer fusing performance. The toner must adhere to the paper, but not to the fuser roll. Improper release of the toner from the fuser roll causes hot offset (ghost images), hollow character defects (lighter inside of large dark areas), and paper wrap (paper jam in fuser). Release of the toner from the fuser roll is determined by the interfacial properties of the toner against the roll. In the past, fuser rolls were impregnated with silicone oil to provide release. This results in a fuser roll with a limited useful life. Modern toner formulations incorporate about 4 wt % of a wax internal release agent. Figure 10(c) shows the viscosity as a function of temperature for a laser printer toner and for polypropylene (PP) and polyethylene (PE) used as internal release agents. The low melt viscosity of the wax allows it to be dispersed in the toner resin during compounding. Since the wax is incompatible with the toner resin, it remains as a dispersed phase. Some of the wax is present on the surface of the toner particles during fusing, which lowers the surface energy of the melt and provides the release.

### Rapid Prototyping

Conventional printing of computer output is two-dimensional. Along with the advent of three-dimensional images to visualize data or the mechanical drawings of machine parts, three-dimensional printing techniques are being developed. An emerging technology for three-dimensional printing, referred to as rapid prototyping (RP), utilizes extrusion and bonding of thermoplastic fibers to construct a three-dimensional output of the image.<sup>11</sup> Among the requirements for the RP thermoplastic material are a melting temperature between 70 and 150°C, no toxicity or volatiles, and specific melt flow properties. In the RP system, a polymer fiber is extruded from a die. Movement of the die and/or table are synchronized with the extrusion to form the three-dimensional object. Fibers are extruded on top of one another to form a wall, side by side to form a

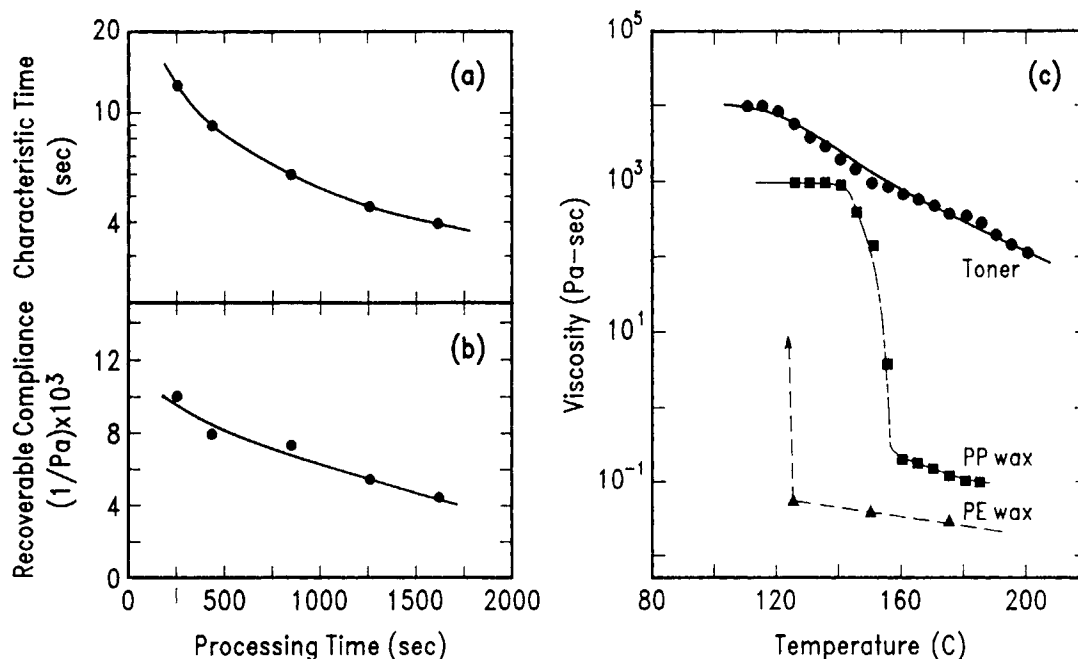


**Figure 10** (a) The characteristic time; (b) recoverable compliance at 160°C as a function of processing time of a toner resin in an internal mixer; (c) viscosity as a function of temperature for laser printer toner and two commonly used wax internal release agents, PP and PE.

shelf, or stretched across gaps to form bridges. The melt flow properties must be such that the shelves and bridges do not sag, and the elastic recovery must be low enough so that the walls do not curl. One rheological test which provides a measure of these properties is the creep and recovery test. In this test, a step stress was applied for 30 s and then removed. The creep compliance during this time and for 30 s following the removal of stress was recorded to characterize two polymers. The performance of the same two polymers was also evaluated in the RP system. The creep and recovery curves are shown in Figure 11. Polymer B had a higher viscosity than did polymer A, while polymer A retained less permanent set than did polymer B. In the RP evaluation, polymer A had lower curl while polymer B showed better bridging and shelving. Creep and other melt rheological tests along with flow modeling are being employed to study the relation between melt properties and performance and to develop new RP polymer materials.

### Cathode Paste

Portable electronic devices and tools are a growing world market. Currently, limitations arise due to the

weight and lifetime of the batteries. Numerous research efforts are underway to develop lighter and higher-energy density rechargeable batteries for portable devices. Among the candidate systems, one of the most promising battery technologies is based on lithium with a solid polymer electrolyte and a composite matrix cathode. This technology has demonstrated feasibility in laboratory test cells. One remaining challenge is the processing of thin films of the battery components on a large scale in manufacturing. The ability to coat such thin films is dominated by the fluid's rheological properties during processing. Specification and control of the rheological properties will play a key role in the success of the rechargeable lithium battery industry. A typical film stack for a rechargeable lithium battery is described as follows<sup>12</sup>: The substrate is polyester film such as that used for magnetic recording tape. The substrate is coated with a metal film on one side for contact to the electrodes. A polymer composite paste coating 10–20  $\mu\text{m}$ -thick forms the cathode. A solid polymer electrolyte such as poly(ethylene oxide) (PEO) and  $\text{LiClO}_4$  10–50  $\mu\text{m}$  thick is coated on the cathode. These films are joined with another metallized polyester film coated with the 25–75  $\mu\text{m}$ -thick Li anode.

Film thickness tolerances are on the order of  $\pm 5\%$ , with no pinholes. The non-Newtonian properties of the cathode paste must be controlled to obtain reproducible films. Typical cathode paste is a highly filled suspension of conductive carbon black particles, vanadium pentoxide particles, PEO binder, and a volatile solvent. The filler concentration should be as high as possible, since the vanadium pentoxide stores the Li ions and the carbon black conducts the electrons. The limitation on the filler content is the thixotropy of concentrated particle suspensions. The initial, increasing stress, portion of a thixotropic loop test on several cathode pastes measured using a stress rheometer is shown in Figure 12. The yield stress is given by the intersection of the data with the vertical axis, and the viscosity is the slope. The viscosity of the pastes are comparable to one another, with the primary difference being the yield stress. The paste with the highest yield stress was too thick to coat, while the paste with the lowest yield stress was too runny. The three pastes with intermediate values of the yield stress exhibited acceptable coating performance.

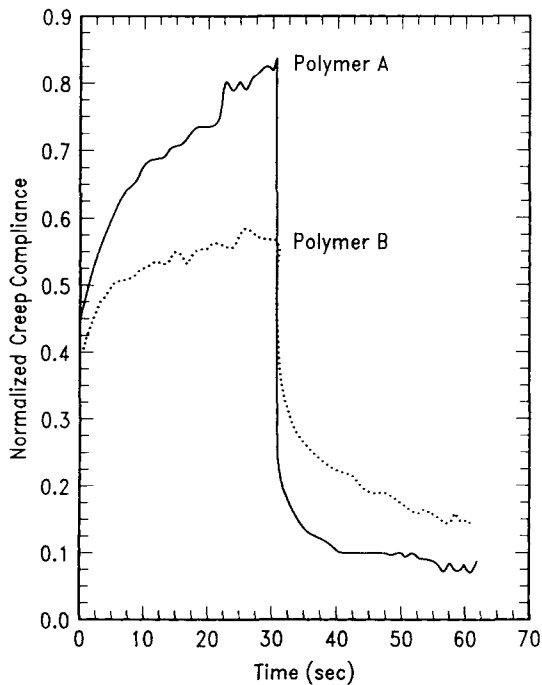


**Figure 11** The creep and recovery curves for two polymer material candidates for use in a rapid prototyping system.

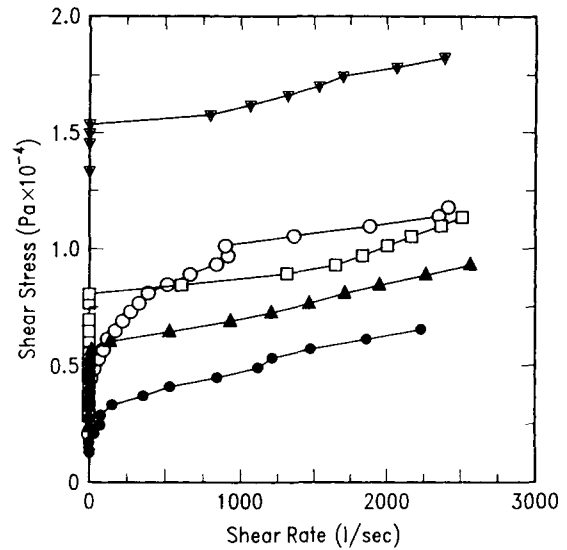


**Figure 12** Thixotropic loop test results used to determine the yield stress and viscosity of lithium battery cathode pastes. Different symbols indicate separately prepared formulations.

## CONCLUSIONS

Applications of rheology to a broad spectrum of materials that are vitally important to the computer industry were presented. Liquid crystal polymers were studied for use as circuit cards. Solder paste rheology was related to screen printing performance. A new photosensitive polymer dielectric formulation was shown to be stable during storage. In the area of hot-melt adhesives, rheological tests played a key role in developing a blend with improved melt-flow properties and solubility. Time-temperature superposition was employed to estimate magneto-optical recording disk lifetime from accelerated life test data. In magnetic recording, the effect of the wet/dry cycling on spindle bearing grease was investigated. The low-temperature rheological properties of magnetic recording disk lubricants was measured to explore their response at high shear rates. Rheological principles were applied to develop a new rheomagnetic apparatus for measuring the dispersion quality of magnetic particle suspensions used in magnetic tape and disk coating. The role of processing time and wax internal release agents in fusing performance of laser printer toner was determined. Exploratory studies on new materials for rapid prototyping and for lithium batteries were described. Overall, rheology is essential to the characterization and development of new materials for the computer industry.

The author is grateful to his colleagues for their assistance and encouragement throughout this work.

## REFERENCES

1. D. S. Kalika, D. S. Giles, and M. M. Denn, *J. Rheol.*, **34**(2), 139-154 (1990).
2. T. E. Karis, O. O. Park, and D. Y. Yoon, *J. Rheol.*, **36**(8), 1587-1603 (1992).
3. J. Frazier and T. Karis, in *Proceedings of the 1991 International Symposium on Microelectronics*, ISBN00930815-29-1, 1991, pp. 228-234.
4. H. Nishigawa, K. Suzuki, T. Kikuchi, and H. Satou, *IEEE Trans. Compon. Hybrids Manuf. Technol.*, **13**(4), 775-779 (1990).
5. Y. Yamaguchi, K. Igarashi, H. Tabata, and H. Suzuki, *IEEE Trans. Compon. Hybrids Manuf. Technol.*, **9**(4), 370-373 (1986).
6. R. Mas and A. Magnin, *J. Rheol.*, **38**(4), 889-908 (1994).
7. V. J. Novotny, T. E. Karis, and N. W. Johnson, *J. Tribol.*, **114**, 61-67 (1992).
8. T. M. Kwon, M. S. Jhon, and T. E. Karis, *Adv. Info. Storage Syst.*, **4**, 87-101 (1992).
9. M. J. Shah, T. E. Karis, and G. M. Cuka, *AIChE J.*, **37**(3), 394-402 (1991).
10. T. E. Karis, C. M. Seymour, and M. S. Jhon, *Polym. Eng. Sci.*, **31**(2), 99-103 (1991).
11. G. Taubes, *IBM Res. Mag.*, **2**, 18-21 (1994); *Mach. Design*, **April 4**, 26 (1994).
12. G. P. Bierwagen, *Electrochim. Acta*, **37**(9), 1471-1478 (1992).

Received January 19, 1995

Accepted August 23, 1995